2000 years of annual ice core data from Law Dome, East Antarctica

Lenneke M. Jong[1,2], Christopher T. Plummer[2], Jason L. Roberts[1,2], Andrew D. Moy[1,2], Mark A. J. Curran[1,2], Tessa R. Vance[2], Joel Pedro[1,2], Chelsea Long[2], Meredith Nation[1,2], Paul A. Mayewski[3], and Tas D. van Ommen[1,2]

[1]Australian Antarctic Division, Department of Agriculture, Water and Environment, Kingston, Tasmania, Australia
[2]Australian Antarctic Program Partnership, Institute of Marine and Antarctic Studies, University of Tasmania, Hobart, Tasmania, Australia
[3]Climate Change Institute, University of Maine, Orono, ME, USA

Correspondence: Lenneke Jong (lenneke.jong@awe.gov.au)

Abstract. Ice core records from Law Dome in East Antarctica collected over the the last three decades, provide high resolution data for studies of the climate of Antarctica, Australia and the Southern and Indo-Pacific Oceans. Here we present a set of annually dated records of trace chemistry, stable water isotopes and snow accumulation from Law Dome covering over the period from -11 to 2017 CE (1961 to -66 BP 1950), as well as the level 1 chemistry data from which the annual chemistry records are derived. This dataset provides an update and extensions both forward and back in time of previously published subsets of the data, bringing them together into a coherent set with improved dating. The data are available for download from the Australian Antarctic Data Centre at https://doi.org/10.26179/5zm0-v192.

1 Introduction

Ice core records from Law Dome in East Antarctica collected over the past four decades have provided high resolution proxy data for studies of Southern Hemisphere climate over the past 2000 years (e.g. (Stenni et al., 2017)). Law Dome is a small ice cap on the coast of East Antarctica (Fig. 1), bounded by the Totten and Vanderford glaciers separating it from the main ice flow from the interior of the East Antarctic ice sheet. It has a maritime climate influenced by large weather systems originating from the Southern Ocean (Bromwich, 1988; Udy et al., 2021), with orographic influence resulting in a snowfall gradient across the dome from east to west with higher annual snowfall to the eastern side (Pfitzner, 1980). The high snowfall accumulation rate is predominantly uniform throughout the year (van Ommen and Morgan, 1997), allowing for ice core records of annual to seasonal resolution which make suitable proxy records of Southern Hemisphere climate. In particular, it provides high resolution records of the Pacific and Indian sectors of the Southern Ocean, where there are limited historical or instrumental observations. Ice cores have been collected from various sites on Law Dome and have been shown to record regional, hemispheric and global records of past climate over the common era. Studies from Law Dome ice cores have included measurements of gases trapped within ice to investigate past atmospheric composition (Etheridge et al., 1998; Rubino et al., 2019), and stable isotopes of water have been used to assess southern Indian Ocean variability (Masson-Delmotte et al., 2003) and in large compilations of past global temperature variability reconstruction (Emile-Geay et al., 2017). Proxies derived from annually dated ice core records from Law Dome have been used to reconstruct climate modes such as El Niño-Southern Oscillation (ENSO) and the

Interdecadal Pacific Oscillation (IPO) (Vance et al., 2015) and have been used as proxy records of Australian rainfall (van
25 Ommen and Morgan, 2010; Vance et al., 2013), for evaluation of solar and meteorological influences on the ^{10}Be solar activity
proxy (Pedro et al., 2011a, b, 2012), volcanic activity (Plummer et al., 2012) and sea ice extent (Curran et al., 2003).

This collection of records supersedes all previously released versions of data from the Dome Summit South (DSS) site on
Law Dome, with the composite record described here forming the best continuous record available, with improved subannual
dating. We provide trace chemistry, stable water isotopes and snow accumulation, with two levels available for some datasets.
30 Level 1 data consists of quality controlled trace chemistry data for chloride (Cl^-), sodium (Na^+), magnesium (Mg^{2+}), calcium
(Ca^{2+}), potassium (K^+), sulphate (SO_4^{2-}), nitrate (NO_3^-) ions, at this time level 1 stable water isotope data is not included.
Level 2 datasets are derived from the level 1 products, with annual averages provided for each chemical species, $\delta^{18}O$ and
snow accumulation as well as seasonal sea salts as examples of what we believe to be the most suitable method for each data
stream as well as details of any limitations which should be considered in their application of further research.

35 Further visits to this site for collecting ice cores is expected as part of an ongoing monitoring project, with subsequent
updates to this record when ice cores become available for analysis. This publication provides a reference point for the full
suite of data, with links to versioned and updated data publicly available for download from the Australian Antarctic Data
Centre at https://doi.org/10.26179/5zm0-v192. Note that in the text of this manuscript we use years CE for dates as the more
natural dating scale, and to be consistent with the naming of some cores using the year or season in which they were drilled.
40 The datasets available for download provide years in both CE and BP 1950 scales and we use BP 1950 (i.e. years before 1950
CE) for plotting of data in figures here.

2 Methods

Drilling campaigns

The DSS site is located approximately 4.7 km SSW from the dome summit (Morgan et al., 1997). The drill sites of the four
45 cores included in this composite record are all located within approximately 1 km of each other, with their relative locations
shown in Figure 1(c). Future visits to the site are planned to ensure the record continues to be updated. A summary of the
details of the drilling campaigns is found in Table 1, with more detailed description of the original drilling site by Morgan et al.
(1997).

Core	Drilling period (CE)	Drill type	Diameter (mm)	Length (m)	Co-ordinates
DSS1617	10/02/2017	Electromechanical (Eclipse)	80	30	66° 46'26.1"S 112° 48'41.82"E
DSS99	20/02/00–06/3/00	Thermal (Horace)	120	125.26	66°46'14"S 112°48'25"E
DSS97	28/10/97–26/11/97	Electromechanical (Eclipse)	82	270	66°46'38"S 112°48'41"E
DSSMain	1988–93	Electromechanical (Istuk)	100	1200	66°46'11"S 112°48'25"E

Table 1. Details of the drilled cores used in this composite record. Locations of each of the individual cores are also shown in figure 1

Earth System
Science
Data
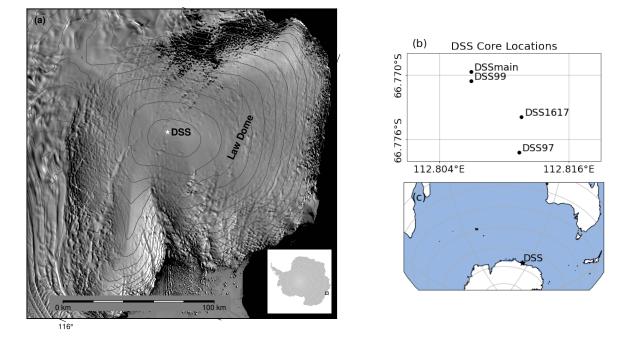
Open Access

Discussions

Figure 1. (a) Location of DSS ice core site on Law Dome, East Antarctica. Background image is MODIS Mosaic of Antarctica Scambos et al. (2007). (b) Relative locations of the 4 individual drill sites used in this record. (c) Regional context of Law Dome.

Dating and age horizon uncertainties

50   The DSS record has been dated using seasonal species variations to define calendar year boundaries, commonly known as annual layer counting. The stable water isotope record is the primary seasonal indicator, with a well-defined maximum of January 10 ± 2.2 days (van Ommen and Morgan, 1997). Confirmation of dating is provided by summer peaking hydrogen peroxide where available, and other chemical markers, such as summer peaking methanesulfonic acid (MSA), non-sea salt sulphate ($nssSO_4^{2-}$) and sulphate/chloride (SO_4^{2-}/Cl^-) ratio, and the winter peaking sea salt species (chloride, sodium (Na^+),

55   magnesium (Mg^+)). Layer counting of the DSS record between 1300 to 1995 CE was previously completed by Palmer et al. (2001b) and verified and extended to cover over 2000 years by Plummer et al. (2012). The DSS record currently spans -11 to 2017 CE with the addition of the DSS1617 core, dated unambiguously from 1989 to 2017 CE. The timescale from Plummer et al. (2012) has been updated by refining the annual layer placement, assisted by new water isotope analysis, and by applying a stricter error counting protocol. The number of years counted has not changed, however the error estimate has increased in

60   the oldest part of the record to +20/-7 at -11 CE, where this date may be up to 20 years older or 7 years younger (-31 to -4 CE) as shown in Fig. 2. Where evidence for a year horizon was not clearly identifiable in the primary seasonal indicators or only weakly supported by confirmatory species, it was not counted. When the majority of (but not all) seasonal indicators show evidence of a year these were counted. Both cases contribute to the total uncertainty estimate. The asymmetrical uncertainty reflects the greater likelihood of just one or two seasonal species indicating a year. We consider this to be a conservative
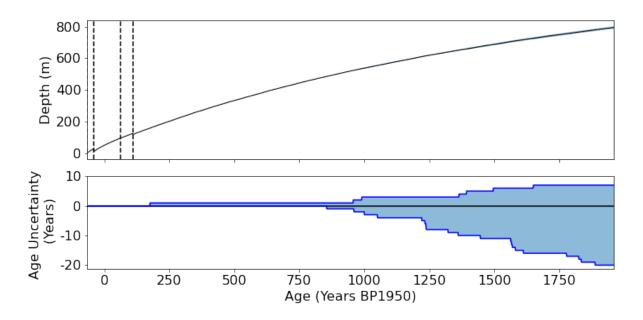
Figure 2. (a) Age at depth for the composite record. Steps in the curve correspond to boundaries between cores, as they were drilled years apart. (b) Accumulated age uncertainties over the 2000 years of data.

65 estimate that represents the extreme error, and is biased toward undercounting. Intra-annual dating of individual sample depths is determined by interpolation between the layer counted annual horizon depths.

We take a conservative approach to calculating the age horizons and uncertainties. The depth of the top of each 1m length of drilled core is locked to the top of the bag as recorded in the drilling logs, so uncertainty from the sample resolution is limited only within each 1m length and errors in depth that may arise from missing or badly fragmented core segments are
70 not cumulative. The sample resolution of chemical measurements is generally much greater than the water isotope sample resolution, hence the larger value is used.

3 Level 1 Datasets

The level 1 datasets have undergone calibration, quality control and post-processing of the raw instrument measurements. The datasets here are obtained from four cores (see Table 1), drilled at the Dome Summit South (DSS 66°46' S 112°48' E) at
75 different times. The main 1196 m (DSSmain) core was drilled between 1987 and 1993. The uppermost 117 m of DSSmain was thermally drilled, and the presence of micro-fractures made it unsuitable for trace ion analysis. Two further shallow cores - DSS97 and DSS99 - were drilled to cover this period for improved data quality. The water stable isotope records from all three cores were used to establish and lock unambiguously the dating and overlap between these cores (Palmer et al., 2001b). The DSS site has been revisited subsequently, with new short cores retrieved to update the DSS record. Previous work from
80 DSS has used other composite records from short cores overlapping with DSS97 (Plummer et al., 2012; Vance et al., 2013;

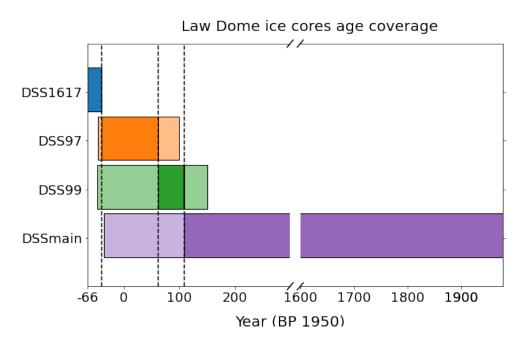**Figure 3.** Periods covered by the cores drilled at DSS at different points in time. Solid colours indicate the periods included in this composite record, transparent colours indicate where other data for the core exists but is not included.

Roberts et al., 2015). The most recent update to the DSS record was DSS1617, a 30 metre core drilled during the 2016/17 CE austral summer season, covering 1989–2017 CE, providing 7 years of overlap with DSS97. Previous composite records for the DSS site have included other short cores which are now no longer used as the periods they covered are now superseded by the longer DSS1617. The periods covered by each of these cores is illustrated in Fig. 3. Where we have a choice of cores, we have typically selected records to avoid the upper most annual cycle of any core (where the friability of surface snow and firn can result in core sections that are more easily compromised during core processing) and to use long, continuous sections from single cores where possible.

The stable water isotope (δ^{18}O) record is sampled at 10–50 mm resolution, with finer physical sampling as annual layers thin with depth. Level 2 annual mean data is provided, however the level 1 datasets of stable water isotopes are not provided at this time but will be published in the future with a manuscript currently in preparation. To assist with dating, sections of cores were measured for hydrogen peroxide at an average resolution of 50 mm as described by van Ommen and Morgan (1996). Discrete chemistry samples were prepared using the clean techniques described by Curran and Palmer (2001). Cores DSS1617, DSS99, DSS97 and DSSmain to 402 m (1300 CE) were sampled at an average resolution of 50 mm, providing up to 60 samples per year in the near-surface firn. Due to a sampling error, a section of DSSmain from 251–273 m (1611–1568 CE) was sampled for chemistry at 100 mm resolution, however isotope and peroxide measurements are available at 50 mm resolution to maintain dating integrity. Beyond 402 m, sample resolution changed to 30 mm and beyond 578 m (979 CE), resolution changed to 25

mm to offset the effects of layer thinning on seasonality. Column headings for the age horizons data file are shown in Appendix B1.

3.1 Trace Ion Chemistry

100 Ice core samples have been analysed using ion chromatography for chloride (Cl^-), sodium (Na^+), magnesium (Mg^{2+}), calcium (Ca^{2+}), potassium (K^+), sulphate (SO_4^{2-}), nitrate (NO_3^-) and methanesulfonic acid (MSA^-). Analytical methods have been modified and updated over the course of the analysis, and are summarised as follows. DSSmain from 117–402 m was analysed using the methods of Buck et al. (1992) at the University of New Hampshire. DSS99, DSS97, and DSSmain from 402–819 m were analysed according to the methods of Curran and Palmer (2001). The DSSmain section 819–829 m was

105 analysed with the methods described by Plummer et al. (2012). The most recent analysis, DSS1617, was analysed according to Plummer et al. (2012) with the exception of the cation analytical column being changed to an Ionpac CS19 for improved detection and peak resolution of magnesium and calcium. Comparison of the analysis methods of Curran and Palmer (2001) and Buck et al. (1992) were discussed by Palmer et al. (2001b), and showed no significant difference. A comparison of the technique used by Plummer et al. (2012) and Curran and Palmer (2001) similarly found no significant differences.

110 A number of species that were measured on parts of the core are not included in this dataset. MSA was not measured on a significant portion of the record. Additionally, deeper sections of the MSA record suffer from unquantified losses from storage prior to analysis (Roberts et al., 2009). The potassium and calcium records are incomplete and suffer issues with poor detection in some older analyses. Additionally, some sections of the DSSmain calcium record appear to have been affected by dust from storage in a concrete floored freezer. Due to these quality concerns, the potassium and calcium records are not discussed further.

115 For the remaining datasets we provide, for each chemical species, the concentration for each sample used in the composite record, an ID corresponding to the drilled core it was obtained from, the top and bottom depths of each sample and the corresponding age.

Species	Mean (μEqL^{-1})	Variance ((μEqL^{-1})^2)	Skewness	Kurtosis
chloride	4.25	13.26	3.06	25
nitrate	0.37	0.06	7.37	145.66
sulphate	0.77	0.17	3.17	25.11
sodium	3.58	10.98	3.50	35.06
magnesium	0.83	0.45	2.24	11.82
non-sea-salt sulphate	0.46	0.16	2.58	29.13

Table 2. Summary statistics for the level 1 data for each analysed species.

Statistical analysis was performed to examine the consistency in the chemistry data obtained from the different cores within the composite, even where there is little or no overlapping data. As the concentrations of trace ions in the ice may depend on

120 the accumulation rate, we have analysed the cores for epochs of approximately constant accumulation rate, and only compared sections which have similar (but not identical) accumulation rates. The detailed results of this analysis shows that the distribu-
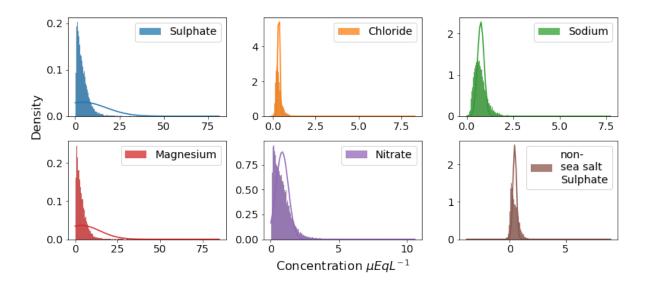
Figure 4. Histogram of the distributions of the level 1 trace chemistry data. Histogram of the concentration of each chemical species, with Normal probability distribution function overlaid, illustrating the non-Gaussian distribution of several of the analytes.

tions of the chemical species concentrations in the different cores are similar in epochs of comparable snow accumulation rate. The results and details of the analysis performed is found in Appendix A.

3.2 Density

125 The firn densification in this region of Law Dome was established from density measurements taken from several cores in the vicinity of DSS. Samples were prepared from dry drilled cores or from melt free interior of thermally drilled cores and were either machined to cylinders on a lathe or pressed from softer firn to a precise volume.

An empirical fit to the firn density profile with depth was presented in van Ommen et al. (1999). Specifically the density (ρ, in $\mathrm{kg\,m^{-3}}$) is fitted as a compound function of depth (z, in m) as

$$130 \quad \rho(z) = 917 - 147.55 \exp\left(-\frac{z}{7.1504}\right) + \begin{cases} 4.2826z - 371.56 & \text{if } z < 56.972 \\ -648.65 \exp\left(-\frac{z}{35.034}\right) & \text{if } z \geq 56.972 \end{cases} \tag{1}$$

The density observations and empirical fit are shown in Figure 5.

Ice Equivalent Depths

For some derived data products (e.g. snow accumulation history) it is useful to be able to remove the effects of firn densification. One common method is to utilise "ice equivalent depths" that represent the depth of a column compressed to the same density
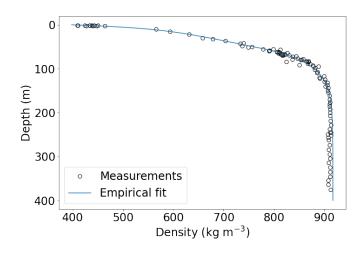
Figure 5. DSS density profile, observations (circles) and empirical fit (solid line, Equation 1)

as glacial ice (density $\rho_{ice} = 917 \, \mathrm{kg} \, \mathrm{m}^{-3}$) and same cross-sectional area, with the same mass as the firn column. Algebraically,
the ice equivalent depth ($\mathcal{Z}$) is given by

$$\mathcal{Z}(z) = \int_0^z \frac{\rho(\eta)}{\rho_{ice}} d\eta = \begin{cases} 0.5948z + 0.002335z^2 + 1.1505 \exp(-z*0.1399) - 1.1505 & \text{if } z < 56.972 \\ z + 1.1505 \exp(-0.1399z) + 24.7817 \exp(-0.02854z) - 21.5316 & \text{if } z \geq 56.972 \end{cases} \tag{2}$$

4 Level 2 datasets

The Level 2 datasets are derived from the Level 1 datasets above. Those presented here have largely been previously published
or included in large data compilations but are now updated, with improved dating of the core. Where there are differences
between the versions, these are remarked upon here. These Level 2 derived datasets can be considered as examples of best
practise for utilising the Level 1 data. A plot of the timeseries for all level 2 datasets is shown in Figure 6.

4.1 Annual stable water isotopes

The DSS annual stable water isotope presented here updates and extends the stable isotope record included in Emile-Geay
et al. (2017) and Stenni et al. (2017) using the DSS1617, DSS99, DSS97 and DSSmain cores (see Figure 3), and currently
spans the period -11 to 2016 CE. The previously published annual composite record for DSS, used in Antarctic temperature
reconstructions (Ahmed et al., 2013; Emile-Geay et al., 2017; Stenni et al., 2017), included other short cores which are now no
longer used as the time periods they covered are now superseded by the longer DSS1617. Also, further water isotope analysis
has extended the annual stable water isotope for the DSSmain record from -11 to 174 CE. The record presented here includes
some changes from the previous records due to the new cores, minor changes in the year boundaries and the new analysis
data. Annual averages are calculated using the year boundaries defined by the summer peak in δ^{18}O. Changes from previously

8

released records have occurred due to new data being obtained from the newer DSS1617 core as well as new analysis at depth from the original DSSmain core. Minor adjustments have been made to the year/depth horizons and corrections to core flips, sample mishandling and depth errors which have been identified since the last release and have been verified by the chemistry

155   records.

4.2   Annual trace ions

Annual average values are presented here, and the calculation method is species dependent. A winter-centred average is used for winter-peaking species (e.g. sea salts) with the boundaries set at the beginning and end of each calendar year. The summer-centred value is calculated from mid-year to mid-year, and used for the nominally summer-peaking species nitrate and non-

160   sea-salt sulphate. This was done to reduce edge effects where small differences in year boundary placement could have strong effects on summer-peaking species. The non-sea-salt sulphate concentration is calculated according to the method of Palmer et al. (2001a) and has a fractionation correction applied to minimize non-physical negative values. The distributions of the annually averaged records is shown in Figure 7

Appendix B3 contains plots of the time series for each of the measured chemistry species, along with the number of samples

165   used for each annual value, the median value and 2σ threshold (see Figures B1 – B6.

4.3   Seasonal sea salts

Characteristics of seasonal cycles of the different species of ions from the Law Dome ice core has been studied over short time periods (Curran et al., 1998), while annual sea salt data has been used previously for high-precision dating of volcanic events (Palmer et al., 2001b), and used for palaeoclimate studies of atmospheric circulation (Souney et al., 2002).

170   Seasonal sea salt records were originally developed for Vance et al. (2013, 2015) and further used in Crockart et al. (2021); Vance et al. (2021), as proxies for regional climate. Specifically these records are the summer, and warm and cool season sea salt average concentrations. The summer sea salt record was developed as a proxy for rainfall variability and a Western Tropical Pacific ENSO proxy in eastern Australia over the Common Era. This record is the seasonal average of sea salt concentrations between December and March. Variability in concentrations is attributed to synoptic scale changes in the southern Indian Ocean

175   (Udy et al., 2021). The warm (December to May) and cool (June to November) season sea salt concentration averages, which were input timeseries for reconstructing Pacific Ocean decadal variability, specifically the Interdecadal Pacific Oscillation index (Parker et al., 2007; Vance et al., 2015, 2016). These datasets have been extended and undergone improved quality control procedures, as detailed in Vance et al. (2021) and adopted here, which extended the IPO reconstruction.

These seasonal records were derived by binning the quality controlled, dated sea salt data from the level 1 datasets into 12

180   months per year. The salt concentrations were log-transformed to normalize (as sea salt data from Law Dome displays long tails due to high frequency aerosol generation events from synoptic activity in the southern Indian Ocean). After binning, timeseries of seasonal averages (December–March, December–May and June–November) were produced with the following caveats. The level 1 sea salt records were examined in conjunction with the updated isotope records (due to having less stringent ice sample requirements) and field and laboratory logbooks detailing core morphology and ice sample cutting. In some instances,

185 the binned sea salt data was compromised due to either missing ice core material from core breaks or shattered sections, or analytical problems resulting in no data or suspected contamination. If this had occurred, the data in question was removed from the analysis. Where more than one month of data was compromised for the summer sea salt record, or two months for the warm and cool season records, we elected to not include that season in our published timeseries. This results in missing values in the seasonal sea salt timeseries of summer, warm and cool season salt concentrations over the last 2000 years. Timeseries

190 for the summer, warm and cool season sea salts are shown in Figures B9, B10 and B11.

4.4 Annual snow accumulation

Snow accumulation is derived using the year horizons obtained through the layer-counted dating. This record has been previously published in Roberts et al. (2015) and updated here to include the newer DSS1617 core data and the improved dating. We assume steady state for depth profiles of both density (Sorge's law) and the vertical strain rate. To compensate for firn

195 densification effects, the depths for year boundaries (see Appendix B3) have been converted to ice equivalent depths using Equation 2. Annual snow accumulation rates were then estimated using the power-law vertical strain rate method of Roberts et al. (2015), based on the assumption of no long-term trend in snow accumulation rate. The resulting snow accumulation rate is shown in Figure B7, with the long term mean snow accumulation rate of 0.691 ± 0.004 IE m y^{-1}.

5 Summary

200 In this paper we have presented the suite of data covering the last 2000 years from the Law Dome ice cores. This set has been updated from previously published results with improved and extended annual dating. We provide quality controlled trace ion chemistry datasets as well as derived, annualised products. Our aim for this paper has been to provide the community with the most complete and consistent suite of Law Dome for the past 2000 years, and examples of best-practise methods for generating derived datasets such as the annual means. The data sets here supersede all previous releases.

6 Data availability

The dataset described in this manuscript can be accessed at the Australian Antarctic Data Centre under https://doi.org/10.26179/5zm0-v192 (Curran et al., 2021)

Appendix A: Trace Chemistry statistical analysis

Due to only very short overlaps between the various ice cores, there is insufficient data for a reliable direct assessment of the

210 consistency of chemical species between the cores. Therefore, as an alternative, we identify different epochs when we might expect similar distributions, specifically periods of time in ice core A where the average accumulation rate approximately the same as ice core B during a different period of time. Changepoint analysis was performed on the cumulative summation

(CUSUM) of the snow accumulation record to determine different epochs of approximately constant accumulation, a technique that has been used to detect changes in the Law Dome snowfall data by Zheng et al. (2021). The CUSUM simply sums the data

215 anomalies an identifies a step change in the underlying data through changes in the gradient of the CUSUM. The changepoints in the CUSUM gradient were detected using the Ruptures Python package (Truong et al., 2020). We select epochs of the closest mean accumulation value and then compare between the different cores using a Kolmogorov-Smirnov (K-S) and a Welch's t-test (W-T) on the log transformed data for each of chemical species. These two tests provide two different ways to test the populations, with the K-S test not assuming a normally distributed population, while log transforming the data for the W-T test

220 mitigates some of the long tail of the distribution. The epochs that were compared are shown in Figure A1, with a summary of the statistical results in Table A1. Visual inspection was also performed using the empirical cumulative probability distributions of the log transformed concentration data, in Figure A2. Overall, the results shown in Table A1 show the results are broadly consistent across the various ice cores. We would not expect all of the tests to show statistically significance for several reasons: a) the accumulation rates used for the comparisons are as similar as possible, but not identical, b) even if the accumulation rates

225 where identical we would expect variability in the species concentrations (i.e, the correlation with accumulation is not perfect) and c) the presence of surface features such as sastrugi will result in different (but highly correlated) ice core records from ice cores drilled at different locations, even only a few metres apart.

Species	DSS1617		DSS99		DSS97	
	K-S	W-T	K-S	W-T	K-S	W-T
chloride	0.147	-5.032	**0.041**	**0.553**	0.081	-3.737
nitrate	0.094	-2.207	0.089	-3.086	0.382	-22.404
sulphate	**0.080**	2.031	0.143	-4.827	0.097	-5.240
sodium	0.126	-4.428	**0.034**	**0.273**	0.098	-4.718
magnesium	0.156	-2.967	0.088	4.161	0.063	**-1.722**

Table A1. Statistical comparison between DSSmain and the shorter DSS97, DSS99, DSS1617 cores that make up the composite. Tests are performed between segments from cores with the closest average value of snow accumulation, as calculated using the changepoint analysis. D-statistics from the Kolmogorov-Smirnov (K-S) test and Welch's t-test (W-T) in bold indicate species where the p-value is greater than 0.05, indicating that the null hypothesis that both samples are from the same distribution cannot be rejected and hence have a comparable distribution.

Appendix B: Data file headers

The files included in this dataset are held at the Australian Antarctic Data Centre are listed here, with column headings provided

230 for each file.

B1   Age Horizons

The file titled "DSS_2k_age_horizons.csv" contains the depths of the year boundaries for the 2000 years of data, produced using annual layer counting methods as described above.

Date (BP 1950)	Date (CE)	Depth (m)	Core name	min error (years)	max error (years)
-66	2016	1.82	DSS1617	0	0
⋮					⋮
1961	-11	793.887	DSS	20	7

Table B1. Year horizons by depth, with accumulated minimum and maximum errors in age.

B2   Level 1 Chemistry

235 The level 1 datasets provide a depth and age for the top and bottom of each sample as well as concentrations of the measured ions. These are contained in the file titled "DSS_2k_chemistry_level1.csv", with column headings provided for reference here in Table B2.

B3   Level 2 data

Two CSV format text files are provided for the Level 2 data sets, "DSS_2k_winter_centred.csv" and "DSS_2k_summer_centred.csv"
240 which contain the annually averaged datasets as described above in Section 4. Column headings are provided for reference here in Tables B3 and B4.

Author contributions. All the authors were involved in the generation of the dataset, through collection, analysis, quality control and dating. LMJ co-ordinated the compilation of the data and led the writing of the manuscript with contributions from all the other authors.

Competing interests. The authors declare that they have no conflict of interest.

References

Ahmed, M., Anchukaitis, K. J., Asrat, A., Borgaonkar, H. P., Braida, M., Buckley, B. M., Büntgen, U., Chase, B. M., Christie, D. A., Cook, E. R., Curran, M. A., Diaz, H. F., Esper, J., Fan, Z. X., Gaire, N. P., Ge, Q., Gergis, J., González-Rouco, J. F., Goosse, H., Grab, S. W., Graham, N., Graham, R., Grosjean, M., Hanhijärvi, S. T., Kaufman, D. S., Kiefer, T., Kimura, K., Korhola, A. A., Krusic, P. J., Lara, A., Lézine, A. M., Ljungqvist, F. C., Lorrey, A. M., Luterbacher, J., Masson-Delmotte, V., McCarroll, D., McConnell, J. R., McKay, N. P., Morales, M. S., Moy, A. D., Mulvaney, R., Mundo, I. A., Nakatsuka, T., Nash, D. J., Neukom, R., Nicholson, S. E., Oerter, H., Palmer, J. G., Phipps, S. J., Prieto, M. R., Rivera, A., Sano, M., Severi, M., Shanahan, T. M., Shao, X., Shi, F., Sigl, M., Smerdon, J. E., Solomina, O. N., Steig, E. J., Stenni, B., Thamban, M., Trouet, V., Turney, C. S., Umer, M., van Ommen, T., Verschuren, D., Viau, A. E., Villalba, R., Vinther, B. M., Von Gunten, L., Wagner, S., Wahl, E. R., Wanner, H., Werner, J. P., White, J. W., Yasue, K., and Zorita, E.: Continental-scale temperature variability during the past two millennia, Nat. Geosci., 6, 339–346, 2013.

Bromwich, D.: Snowfall in high southern latitudes, Reviews of Geophysics, 26, 149–168, 1988.

Buck, C. F., Mayewski, P. A., Spencer, M. J., Whitlow, S., Twickler, M. S., and Barrett, D.: Determination of major ions in snow and ice cores by ion chromatography, J. Chromatogr. A, 594, 225–228, https://doi.org/10.1016/0021-9673(92)80334-Q, 1992.

Crockart, C. K., Vance, T. R., Fraser, A. D., Abram, N. J., Criscitiello, A. S., Curran, M. A., Favier, V., Gallant, A. J., Kittel, C., Kjær, H. A., Klekociuk, A. R., Jong, L. M., Moy, A. D., Plummer, C. T., Vallelonga, P. T., Wille, J., and Zhang, L.: El Niño-Southern oscillation signal in a new east antarctic ice core, Mount Brown South, Clim. Past, 17, 1795–1818, https://doi.org/10.5194/cp-17-1795-2021, 2021.

Curran, M., M., Jong, L., Moy, A., Plummer, C., Roberts, J., Van Ommen, T., and Vance, T.: The Law Dome ice core 2000 year dataset collection, Australian Antarctic Data Centre [dataset], https://doi.org/doi:10.26179/5zm0-v192, "Ver. 1 Accessed Nov. 19, 2021", 2021.

Curran, M. A. and Palmer, A. S.: Suppressed ion chromatography methods for the routine determination of ultra low level anions and cations in ice cores, Journal of Chromatography A, 919, 107–113, https://doi.org/https://doi.org/10.1016/S0021-9673(01)00790-7, 2001.

Curran, M. A., Van Ommen, T. D., and Morgan, V.: Seasonal characteristics of the major ions in the high-accumulation Dome Summit South ice core, Law Dome, Antarctica, Annals of Glaciology, 27, 385–390, https://doi.org/10.3189/1998AoG27-1-385-390, 1998.

Curran, M. A. J., Van Ommen, T. D., Morgan, V. I., Phillips, K. L., and Palmer, A. S.: Ice Core Evidence for Antarctic Sea Ice Decline since the 1950s, Science (80-.)., 302, 1203–1206, https://doi.org/10.1126/science.1087888, 2003.

Emile-Geay, J., McKay, N. P., Kaufman, D. S., von Gunten, L., Wang, J., Anchukaitis, K. J., Abram, N. J., Addison, J. A., Curran, M. A., Evans, M. N., Henley, B. J., Hao, Z., Martrat, B., McGregor, H. V., Neukom, R., Pederson, G. T., Stenni, B., Thirumalai, K., Werner, J. P., Xu, C., Divine, D. V., Dixon, B. C., Gergis, J., Mundo, I. A., Nakatsuka, T., Phipps, S. J., Routson, C. C., Steig, E. J., Tierney, J. E., Tyler, J. J., Allen, K. J., Bertler, N. A., Björklund, J., Chase, B. M., Chen, M.-T., Cook, E., de Jong, R., DeLong, K. L., Dixon, D. A., Ekaykin, A. A., Ersek, V., Filipsson, H. L., Francus, P., Freund, M. B., Frezzotti, M., Gaire, N. P., Gajewski, K., Ge, Q., Goosse, H., Gornostaeva, A., Grosjean, M., Horiuchi, K., Hormes, A., Husum, K., Isaksson, E., Kandasamy, S., Kawamura, K., Kilbourne, K. H., Koç, N., Leduc, G., Linderholm, H. W., Lorrey, A. M., Mikhalenko, V., Mortyn, P. G., Motoyama, H., Moy, A. D., Mulvaney, R., Munz, P. M., Nash, D. J., Oerter, H., Opel, T., Orsi, A. J., Ovchinnikov, D. V., Porter, T. J., Roop, H. A., Saenger, C., Sano, M., Sauchyn, D., Saunders, K. M., Seidenkrantz, M.-S., Severi, M., Shao, X., Sicre, M.-A., Sigl, M., Sinclair, K., St. George, S., St. Jacques, J.-M., Thamban, M., Kuwar Thapa, U., Thomas, E. R., Turney, C., Uemura, R., Viau, A. E., Vladimirova, D. O., Wahl, E. R., White, J. W., Yu, Z., Zinke, J., and Zinke, J.: A global multiproxy database for temperature reconstructions of the Common Era, Sci. Data, 4, 170 088, https://doi.org/10.1038/sdata.2017.88, http://www.nature.com/articles/sdata201788, 2017.

Earth System
Science
Data

Open Access

Discussions

Etheridge, D. M., Steele, L. P., Francey, R. J., and Langenfelds, R. L.: Atmospheric methane between 1000 A.D. and present: Evidence of anthropogenic emissions and climatic variability, Journal of Geophysical Research: Atmospheres, 103, 15 979–15 993, https://doi.org/https://doi.org/10.1029/98JD00923, 1998.

290 Masson-Delmotte, V., Delmotte, M., Morgan, V., Etheridge, D., van Ommen, T., Tartarin, S., and Hoffmann, G.: Recent southern Indian Ocean climate variability inferred from a Law Dome ice core: New insights for the interpretation of coastal Antarctic isotopic records, Clim. Dyn., 21, 153–166, https://doi.org/10.1007/s00382-003-0321-9, 2003.

Morgan, V., Wookey, C., Li, J., van Ommen, T., Skinner, W., and Fitzpatrick, M.: Site information and initial results from deep ice drilling on Law Dome, Antarctica, J. Glaciol., 43, 3–10, https://doi.org/10.3189/S0022143000002768, 1997.

295 Palmer, A. S., Van Ommen, T. D., Curran, M. A. J., and Morgan, V.: Ice-core evidence for a small solar-source of atmospheric nitrate, Geophys. Res. Lett., 28, 1953–1956, https://doi.org/10.1029/2000GL012207, 2001a.

Palmer, A. S., van Ommen, T. D., Curran, M. A. J., Morgan, V., Souney, J. M., and Mayewski, P. A.: High-precision dating of volcanic events (A.D. 1301-1995) using ice cores from Law Dome, Antarctica, Journal of Geophysical Research: Atmospheres, 106, 28 089–28 095, https://doi.org/10.1029/2001JD000330, http://doi.wiley.com/10.1029/2001JD000330, 2001b.

300 Parker, D., Folland, C., Scaife, A., Knight, J., Colman, A., Baines, P., and Dong, B.: Decadal to multidecadal variability and the climate change background, J. Geophys. Res. Atmos., 112, https://doi.org/10.1029/2007JD008411, 2007.

Pedro, J. B., Heikkilä, U. E., Klekociuk, A., Smith, A. M., Van Ommen, T. D., and Curran, M. A.: Beryllium-10 transport to Antarctica: Results from seasonally resolved observations and modeling, J. Geophys. Res. Atmos., 116, 1–14, https://doi.org/10.1029/2011JD016530, 2011a.

305 Pedro, J. B., Smith, A. M., Simon, K. J., van Ommen, T. D., and Curran, M. A. J.: High-resolution records of the beryllium-10 solar activity proxy in ice from Law Dome, East Antarctica: measurement, reproducibility and principal trends, Climate of the Past, 7, 707–721, https://doi.org/10.5194/cp-7-707-2011, https://cp.copernicus.org/articles/7/707/2011/, 2011b.

Pedro, J. B., McConnell, J. R., van Ommen, T. D., Fink, D., Curran, M. A., Smith, A. M., Simon, K. J., Moy, A. D., and Das, S. B.: Solar and climate influences on ice core 10Be records from Antarctica and Greenland during the neutron monitor era, Earth Planet. Sci. Lett., 310 355-356, 174–186, https://doi.org/10.1016/j.epsl.2012.08.038, http://dx.doi.org/10.1016/j.epsl.2012.08.038, 2012.

Pfitzner, M.: The Wilkes Ice Cap project, 1966, ANARE Sci. Rep. 127, Department of Science and Technology, Antarctic Division, 1980.

Plummer, C. T., Curran, M. A. J., van Ommen, T. D., Rasmussen, S. O., Moy, A. D., Vance, T. R., Clausen, H. B., Vinther, B. M., and Mayewski, P. A.: An independently dated 2000-yr volcanic record from Law Dome, East Antarctica, including a new perspective on the dating of the 1450s CE eruption of Kuwae, Vanuatu, Clim. Past, 8, 1929–1940, https://doi.org/10.5194/cp-8-1929-2012, 2012.

315 Roberts, J., Plummer, C., Vance, T., van Ommen, T., Moy, A., Poynter, S., Treverrow, A., Curran, M., and George, S.: A 2000-year annual record of snow accumulation rates for Law Dome, East Antarctica, Climate of the Past, 11, 697–707, https://doi.org/10.5194/cp-11-697-2015, 2015.

Roberts, J. L., Van Ommen, T. D., Curran, M. A. J., and Vance, T. R.: Methanesulphonic acid loss during ice-core storage: Recommendations based on a new diffusion coefficient, J. Glaciol., 55, 784–788, https://doi.org/10.3189/002214309790152474, 2009.

320 Rubino, M., Etheridge, D. M., Thornton, D. P., Howden, R., Allison, C. E., Francey, R. J., Langenfelds, R. L., Paul Steele, L., Trudinger, C. M., Spencer, D. A., J Curran, M. A., van Ommen, T. D., and Smith, A. M.: Revised records of atmospheric trace gases over the last 2000 years from Law Dome, Antarctica, Earth Syst. Sci. Data, 11, 473–492, https://doi.org/10.5194/essd-11-473-2019, https://doi.org/10.5194/essd-11-473-2019, 2019.
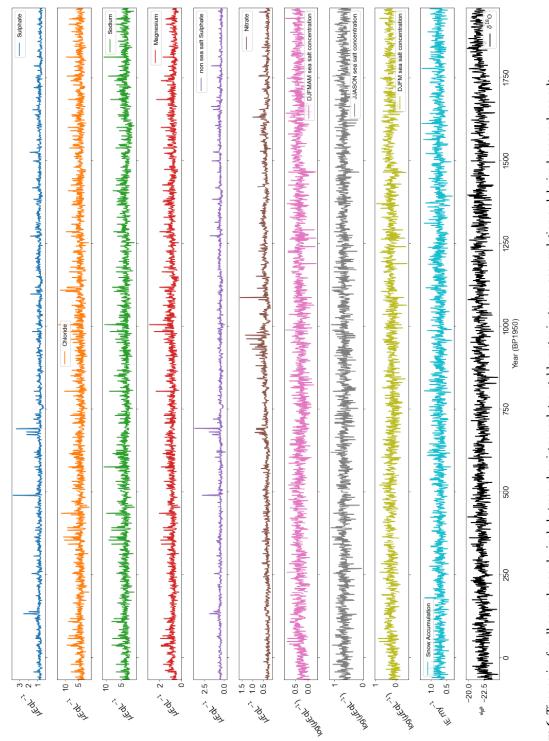
Scambos, T. A., Haran, T. M., Fahnestock, M. A., Painter, T. H., and Bohlander, J.: MODIS-based Mosaic of Antarctica (MOA) data sets:
325   Continent-wide surface morphology and snow grain size, Remote Sens. Environ., 111, 242–257, https://doi.org/10.1016/j.rse.2006.12.020,
       2007.

Souney, J. M., Mayewski, P. A., Goodwin, I. D., Meeker, L. D., Morgan, V., Curran, M. A., Van Ommen, T. D., and Palmer, A. S.: A 700-year
       record of atmospheric circulation developed from the Law Dome ice core, East Antarctica, J. Geophys. Res. Atmos., 107, ACL 1–1–ACL
       1–9, https://doi.org/10.1029/2002JD002104, 2002.

330 Stenni, B., Curran, M. A. J., Abram, N. J., Orsi, A., Goursaud, S., Masson-Delmotte, V., Neukom, R., Goosse, H., Divine, D., van Ommen,
       T., Steig, E. J., Dixon, D. A., Thomas, E. R., Bertler, N. A. N., Isaksson, E., Ekaykin, A., Werner, M., and Frezzotti, M.: Antarctic climate
       variability on regional and continental scales over the last 2000 years, Clim. Past, 13, 1609–1634, https://doi.org/10.5194/cp-13-1609-
       2017, https://doi.org/10.5194/cp-13-1609-2017https://www.clim-past.net/13/1609/2017/, 2017.

Truong, C., Oudre, L., and Vayatis, N.: Selective review of offline change point detection methods, Signal Processing, 167, 107 299,
335   https://doi.org/10.1016/j.sigpro.2019.107299, https://doi.org/10.1016/j.sigpro.2019.107299, 2020.

Udy, D. G., Vance, T. R., Kiem, A. S., Holbrook, N. J., and Curran, M. A. J.: Links between Large-Scale Modes of Climate Variability and
       Synoptic Weather Patterns in the Southern Indian Ocean, Journal of Climate, 34, 883 – 899, https://doi.org/10.1175/JCLI-D-20-0297.1,
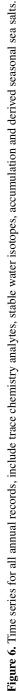   https://journals.ametsoc.org/view/journals/clim/34/3/JCLI-D-20-0297.1.xml, 2021.

van Ommen, T. D. and Morgan, V.: Peroxide concentrations in the Dome Summit South ice core, Law Dome, Antarctica, J. Geophys. Res.
340   Atmos., 101, 15 147–15 152, https://doi.org/10.1029/96JD00838, http://doi.wiley.com/10.1029/96JD00838, 1996.

van Ommen, T. D. and Morgan, V.: Calibrating the ice core paleothermometer using seasonality, Journal of Geophysical Research: Atmo-
       spheres, 102, 9351–9357, https://doi.org/10.1029/96JD04014, 1997.

van Ommen, T. D. and Morgan, V.: Snowfall increase in coastal East Antarctica linked with southwest Western Australian drought, Nat.
       Geosci., 3, 267–272, https://doi.org/10.1038/ngeo761, 2010.

345 van Ommen, T. D., Morgan, V. I., Jacka, T. H., Woon, S., and Elcheikh, A.: Near-surface temperatures in the Dome Summit South (Law
       Dome, East Antarctica) borehole, Annals of Glaciology, 29, 141–144, https://doi.org/10.3189/172756499781821382, 1999.

Vance, T. R., van Ommen, T. D., Curran, M. A. J., Plummer, C. T., and Moy, A. D.: A Millennial Proxy Record of ENSO and Eastern
       Australian Rainfall from the Law Dome Ice Core, East Antarctica, J. Clim., 26, 710–725, https://doi.org/10.1175/JCLI-D-12-00003.1,
       2013.

350 Vance, T. R., Roberts, J. L., Plummer, C. T., Kiem, A. S., and van Ommen, T. D.: Interdecadal Pacific variability and eastern Australian
       megadroughts over the last millennium, Geophys. Res. Lett., 42, 129–137, https://doi.org/10.1002/2014GL062447, 2015.

Vance, T. R., Roberts, J. L., Moy, A. D., Curran, M. A. J., Tozer, C. R., Gallant, A. J. E., Abram, N. J., van Ommen, T. D., Young, D. A.,
       Grima, C., Blankenship, D. D., and Siegert, M. J.: Optimal site selection for a high-resolution ice core record in East Antarctica, Clim. Past,
       12, 595–610, https://doi.org/10.5194/cp-12-595-2016, www.clim-past.net/12/595/2016/http://www.clim-past.net/12/595/2016/, 2016.

355 Vance, T. R., Kiem, Anthony S., J., M., L., Roberts, J. L. R., Plummer, C. T., Moy, A. D., Curran, M. A., and van Ommen, T. D.: Pacific
       decadal variability over the last 2000 years: Implications for climatic risk, In Review, 2021.

Zheng, Y., Jong, L. M., Phipps, S. J., Roberts, J. L., Moy, A. D., Curran, M. A. J., and van Ommen, T. D.: Extending and understanding
       the South West Western Australian rainfall record using a snowfall reconstruction from Law Dome, East Antarctica, Clim. Past, 17,
       1973–1987, https://doi.org/10.5194/cp-17-1973-2021, https://cp.copernicus.org/articles/17/1973/2021/, 2021.
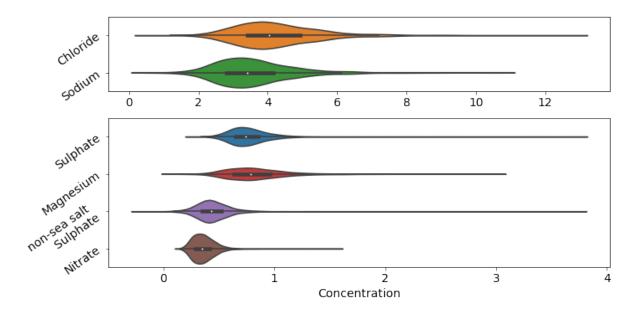
Figure 6. Time series for all annual records, include trace chemistry analytes, stable water isotopes, accumulation and derived seasonal sea salts.

Figure 7. Violin plots showing the median, interquartile range and distribution of the annually averaged trace ions. The chloride and sodium records are separated only for illustrative purposes so that their higher concentrations do not dominate the plots of the other ions.
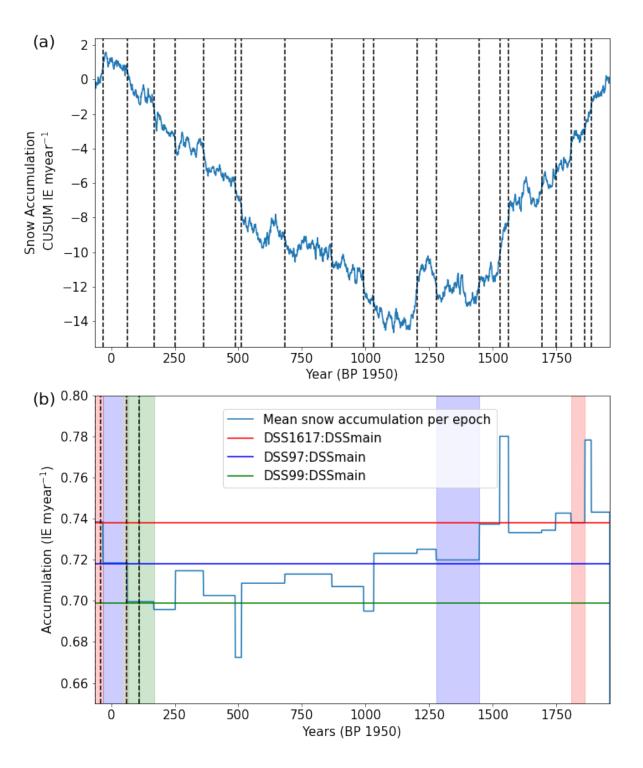
Figure A1. (a) Cumulative sum of the annual snow accumulation rate with detected change points indicated by vertical dashed lines. (b) Average snow accumulation epochs used for chemistry data statistical analysis.

Figure A2. Empirical cumulative distribution functions of the log transformed concentration data for each trace chemistry species. Epochs from DSS1617, DSS99 and DSS97 are each compared against epochs from the DSSmain core with similar, but not identical, snow accumulation rates. Epochs are determined by the changepoint analysis on the CUSUM snow accumulation.

Sample ID	Top depth (m)	Bottom depth (m)	Top Date (BP 1950)	Bottom Date (BP 1950)	Mid Depth Date (BP 1950)	Cl$^-$ (μEqL^{-1})
DSSp1617A-1_9	0.255	0.300	-66.981	-66.953	-66.967	3.967
. . .						. . .
DSS 832-6	793.863	793.888	1960.867	1961.005	1960.936	1.063

Sample ID	NO$_3^-$ (μEqL^{-1})	SO$_4^{2+}$ (μEqL^{-1})	Na$^+$ (μEqL^{-1})	Mg^{2+} (μEqL^{-1})	nssSO$_4^{2+}$ (μEqL^{-1})
DSSp1617A-1_9	0.427	1.572	3.332	0.679	1.281
. . .					. . .
DSS 832-6	0.203	0.598	1.195	0.149	0.494

Table B2. Column headings Level 1 trace ion chemistry data file.

Year (BP 1950)	Year (CE)	Na (μEqL^{-1})	Cl (μEqL^{-1})	Mg (μEqL^{-1})	SO$_4$ (μEqL^{-1})
-66	2016	4.326	4.994	0.844	0.795
⋮					⋮
1961	-11	2.925	3.687	0.46	0.589

Year (BP1950)	Year (CE)	δ^{18}O (‰)	Layer Thickness (m)	Accumulation rate (IE m y^{-1})
-66	2016	-22.5116322040234	0.733355	0.734644
⋮				⋮
1961	-11	-22.1038028786394	0.18	0.662081

Table B3. Winter centred annual data columns included in "DSS_2k_winter_centred.csv" file.

Figure B1. Time series for annually averaged sodium. Solid black line indicates the 2000 year mean value. Dashed black line indicates 2σ value.

Year (BP 1950)	Year (CE)	NO$_3^-$ (μEqL^{-1})	nss$_S$O$_4^{2+}$ (μEqL^{-1})
-66.5	2016.5	NaN	NaN
-65.5	2015.5	0.31	0.453
⋮			⋮
1959.5	-9.5	0.363	0.33
1960.5	-10.5	NaN	NaN

Table B4. Summer centred annual data columns included in "DSS_2k_summer_centred.csv" file.

21

Figure B2. Time series for annually averaged chloride. Solid black line indicates the 2000 year mean value. Dashed black line indicates 2σ value.
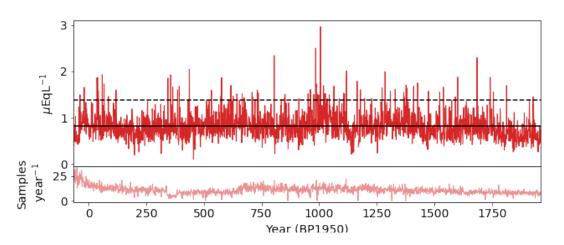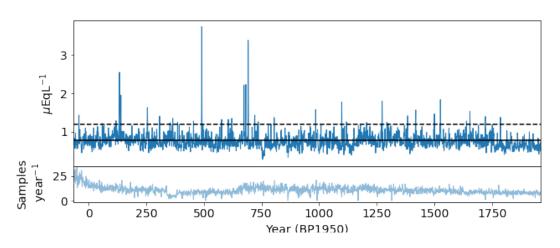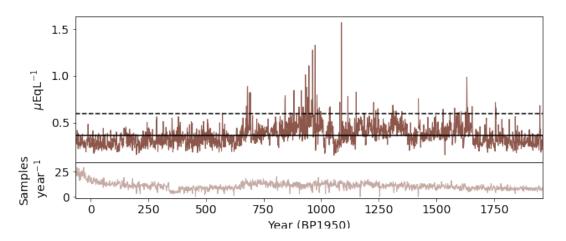

Figure B3. Time series for annually averaged magnesium. Solid black line indicates the 2000 year mean value. Dashed black line indicates 2σ value.
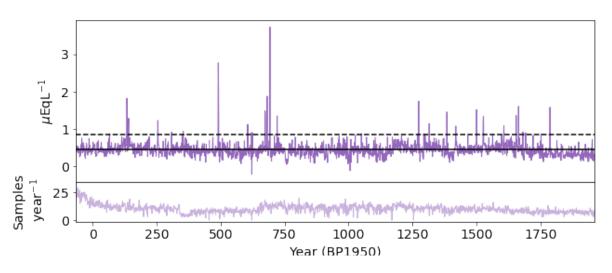
Figure B4. Time series for annually averaged sulphate. Solid black line indicates the 2000 year mean value. Dashed black line indicates 2σ value.
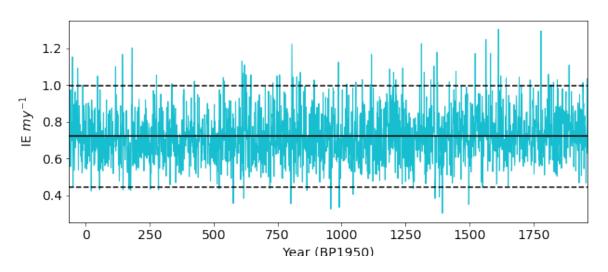

Figure B5. Time series for annually averaged nitrate.Solid black line indicates the 2000 year mean value. Dashed black line indicates 2σ value.

Figure B6. Time series for annually averaged non-sea salt sulphate.Solid black line indicates the 2000 year mean value. Dashed black line indicates 2σ value.

Figure B7. Time series for the annual snow accumulation rate. Solid black line indicates the 2000 year mean value. Dashed black line indicates $\pm 2\sigma$ value.
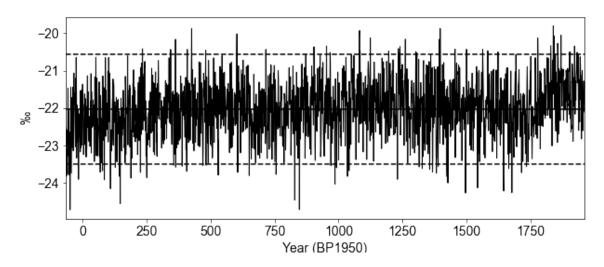
Figure B8. Time series for annually averaged δ^{18}O. Solid black line indicates the 2000 year mean value. Dashed black line indicates $\pm 2\sigma$ value.
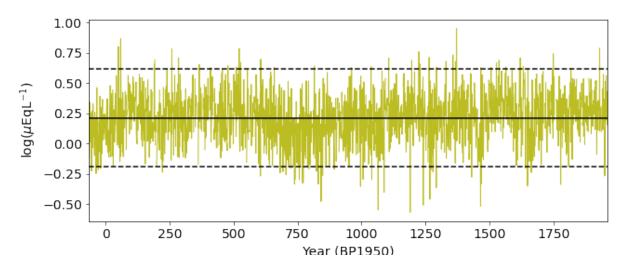

Figure B9. Time series for DJFM (Summer) annual sea salts concentration. Solid black line indicates the 2000 year mean value. Dashed black line indicates $\pm 2\sigma$ value.
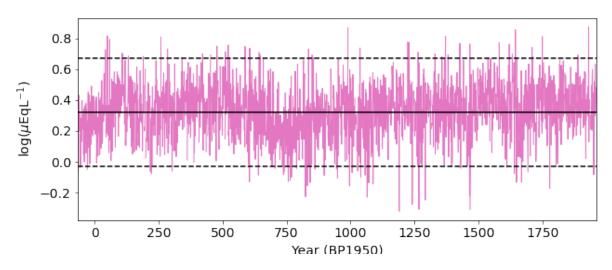
Figure B10. Time series for DJFMAM (warm season) annual sea salts concentration. Solid black line indicates the 2000 year mean value. Dashed black line indicates $\pm 2\sigma$ value.
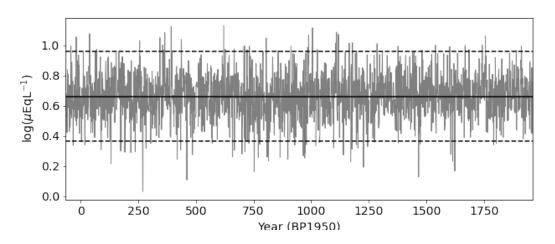

Figure B11. Time series for JJASON (cool season) annual sea salts concentration. Solid black line indicates the 2000 year mean value. Dashed black lines indicates $\pm 2\sigma$ value.